6

Wind Turbines Aerodynamics

J. Lassig[1] and J. Colman[2]
[1]*Environmental Fluid Dynamics Laboratory, Engineering Faculty, National University of Comahue*
[2]*Boundary Layer and Environmental Fluid Dynamics Laboratory, Engineering Faculty, National University of La Plata*
Argentina

1. Introduction

Since the earlier petroleum crisis (decade of 70s), when begun the interest of the aeronautical industry into wind turbines development until the present, 40 years of research and development become in an important design evolution.

At the present we could say that a modern rotor blade design implies some different aerodynamics criteria than used regarding wings and airplane propellers designs.

This is due that their operating environment and operation mode are quite different than airplanes ones. Such differences could be summarized as follows:

1. Flow characteristics of the media where they function
2. Relative movement of the aerodynamic parts regarding free upwind flow

1.1 Environment

Wind turbines are immersed in the low atmospheric boundary layer, characterized by the inherent turbulent nature of the winds and, also, for the presence of dust, sand and insects, which finally ends gluing to the blades surfaces incrementing their roughness.

For the reasons mentioned above, the rotor blade airfoil is submitted to a time and space variation flow, producing on it different superimposed phenomena promoting flow hysteresis, like dynamic stall.

By other way, the wind which transports dust and other particles in the boundary layer, will change the apparent blade roughness and for that reason the airfoils to be used on blade design, should be almost no-sensitive to such roughness changes.

1.2 Operating mode

The second aspect to be considered is the rotor operating mode, because blade turbines have a relative movement regarding upwind flow, with changes at each blade section due the resultant velocity at the blade will be the vector sum between the upwind flow and the tangential rotation.

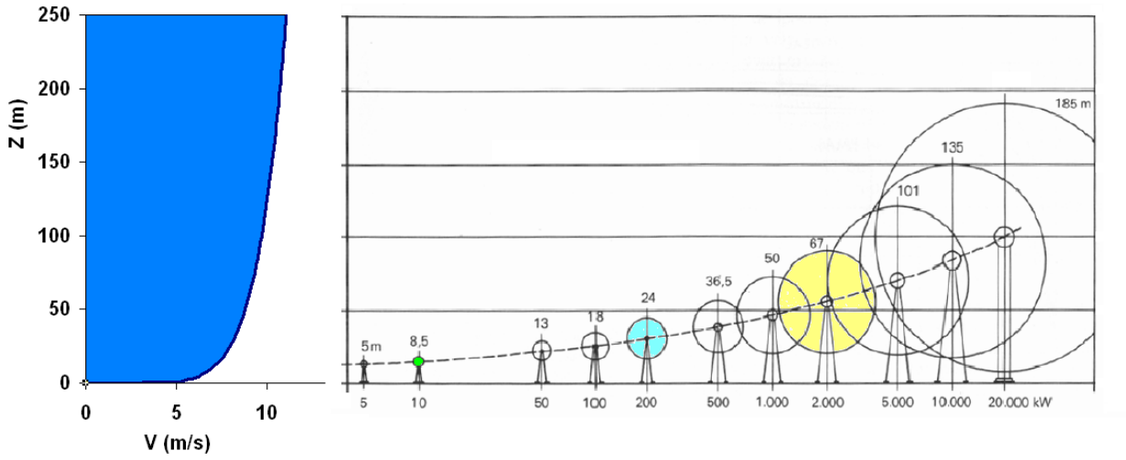

Fig. 1. Typical vertical mean wind velocity distribution in the low atmospheric boundary layer, compared with the rotor size evolution

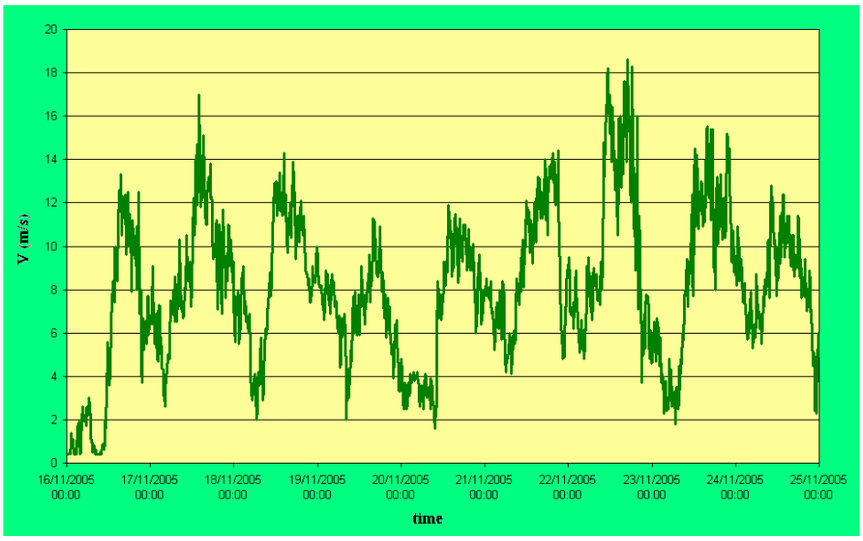

Fig. 2. Wind time variation during a 10 days period, measured in a 30m height tower located at Vavarco town, Neuquen´s Province, Argentina

2. Wind turbines

The energy per unit time transported by the upstream wind, or meteorological power, is defined as:

$$P_m = \frac{1}{2} \cdot \rho \cdot \int_0^\infty f(v) \cdot V^3 dv \tag{1}$$

where *f(v)* is the wind distribution function at the zone to be considered.

That´s the indicative wind power of the potentiality of the zone. In order to quantify it in watts, we must multiply such formula by the area to be considered ($A = \pi \cdot R^2$), achieving by this way the expression for the Available Power:

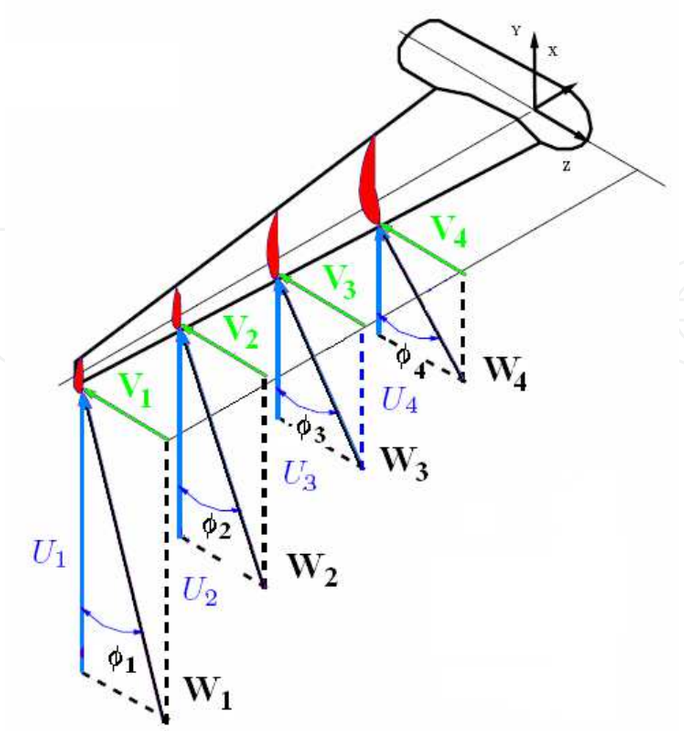

Fig. 3. Resultant flow over rotor blades, being V the mean free upwind velocity, U the tangent velocity, W the resultant and φ the effective pitch angle, measured respect the rotation plane

$$P_d = 1/2 \cdot \rho \cdot V_0^3 \cdot \pi \cdot R^2 \quad (2)$$

In order to extract all that power, by means of the rotor, the wind velocity behind it should be zero and, obviously, that´s impossible. So, we could only extract part of the Available Power being such part the Obtainable Power:

$$P_{obt} = P_d \cdot C_p \quad (3)$$

Where C_p is the rotor´s power coefficient.

2.1 Momentum or Froude´s or Betz´s propeller model

This simply model consists on considerer the rotor as an *actuator disk* integrated by a great number of infinitesimal width needles. The disk rotate when the wind pass trough it. The hypotheses of the model are:

a. Upstream flow is non-rotational, non-viscous and incompressible
b. Air, at the disk rotation plane is rotational, viscous, etc, but will not be considered directly on the calculus.
c. Downstream flow will be non-rotational, non-viscous and incompressible but, due it crossed the disk, the Bernoulli constants will be different upstream and downstream. This constant change is the only factor which "incorporates" part of the true behavior of the flow on crossing the disk plane.

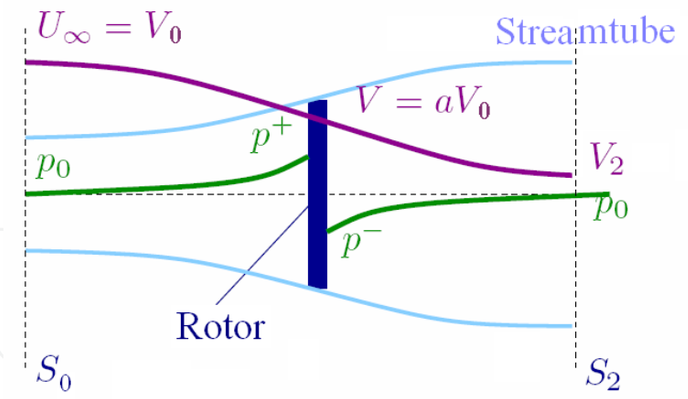

Fig. 4. Expansion stream tube effects, upon the flow through the rotor, producing a downwash velocity reduction (V_2).

The upwind stream tube have a velocity V_0 and, after flow through the rotor plane, part of the kinetic energy is transformed in extracted energy due the rotor, producing a downwind velocity reduction and, so, the stream tube will expand in order to fulfill the continuity equation.

V_0 and V_2 are defined as:

$$V = V_0 (1-a) \tag{4}$$

$$V_2 = V_0 (1-2\,a) \tag{5}$$

Being *a* an axial induction factor, which take into account the stream tube expansion. According that, a non-dimensional Power Coefficient C_p is defined:

$$C_P = \frac{AvailablePower}{1/2 \cdot \rho \cdot V_0^3 \cdot A} \tag{6}$$

$$\textit{Available Power} = \text{Force} \cdot \text{Velocity} = \Delta P.A.V = (P^+ - P^-).A.V = \tfrac{1}{2}.\rho AV(V_0^2 - V_2^2) \tag{7}$$

Using [4] and [5] in the former equation, we obtain:

$$\textit{Available Power} = 2.\rho.A.a(1-a)^2.V_0^2 \tag{8}$$

Then C_P could be expressed as:

$$C_P = 4 \cdot (1-a)^2 \cdot a \tag{9}$$

Taking in account the blades rotation (angular velocity w_d) and that the air, on trespassing the rotor plane, receive also a rotation movement w_w, slightly different than the blade rotation (see Figure 5), we could relate both rotation velocities as

$$w_w = a' \,.\, w_d \tag{10}$$

Being *a´* an rotational induction factor. According all those factors, the expression for the Power Coefficient will be:

$$C_P = 4\,a\,(1-a)^2 \,/\, (1+a') \tag{11}$$

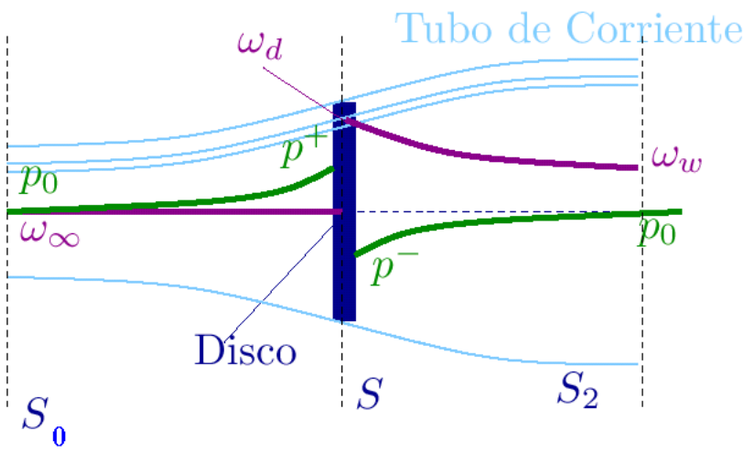

Fig. 5. Stream tube changes, where we could appreciate the rotation effects of the upwind (w_∞), on the rotor plane (w_d) and downwind (w_w)

2.2 Blade element theory

The aerodynamic forces upon the rotor blades could be expressed as functions of lift and drag coefficients and the angle of attack.

In doing so, we divide the blade in a finite but large number of sections (N), denominated blade elements.

The theory is supported by the following assumptions: there aren´t any aerodynamic interaction between each blade element (which is equivalent as assume 2D flow over the blade); the velocity components over the blade along wingspan aren´t take in account; forces upon each blade element are determined by the aerodynamic airfoil characteristics (2D flow). All of these implies, in fact, that the blade´s aspect ratio will be great than 6.

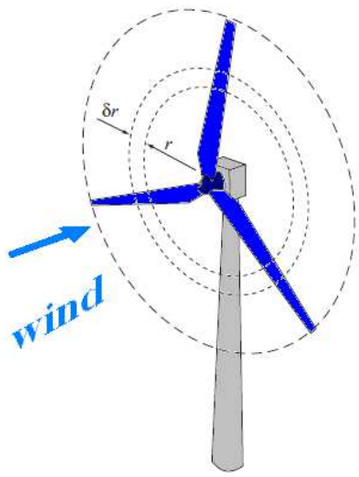

Fig. 6. Blade element of width δr, located at a distance r from the rotor hub. Note the annulus traverse surface due the rotation.

In the blade-element analysis, section lift and drag are normal and parallel to the relative wind, respectively (see Figure 7). It´s consider a turbine blade sliced in N elements of chord C, width dr, with geometric pitch angle ß between rotor´s rotation plane and the chord line for zero lift.

Both, chord and pitch, will vary along blade wingspan. If Ω is the angular velocity and V_∞ the mean upstream wind velocity, the angular component of the resultant velocity at the blade will be:

$$(1 + a') \, \Omega \, . \, r \tag{12}$$

and the axial component:

$$(1- a)V_\infty. \tag{13}$$

So, the relative velocity in the blade plane will be expressed as:

$$W = \sqrt{V_\infty^2(1-a)^2 + \Omega^2 r^2 (1+á)^2} \tag{14}$$

This relative velocity forms an angle α respect the rotation plane.

From definitions and showing Figure 7, we could write:

$$\tan\phi = \frac{V_\infty(1-a)}{\Omega r(1-á)} = \frac{(1-a)}{(1-á)\lambda_r} \tag{15}$$

Net force at each blade-element, normal to the rotation plane, could be expressed as

$$\delta F = r(\delta L \cdot \cos\phi + \delta D \cdot \sin\phi) \tag{16}$$

Being δL and δD the differential lift and drag, respectively, and L and D the total lift and drag.

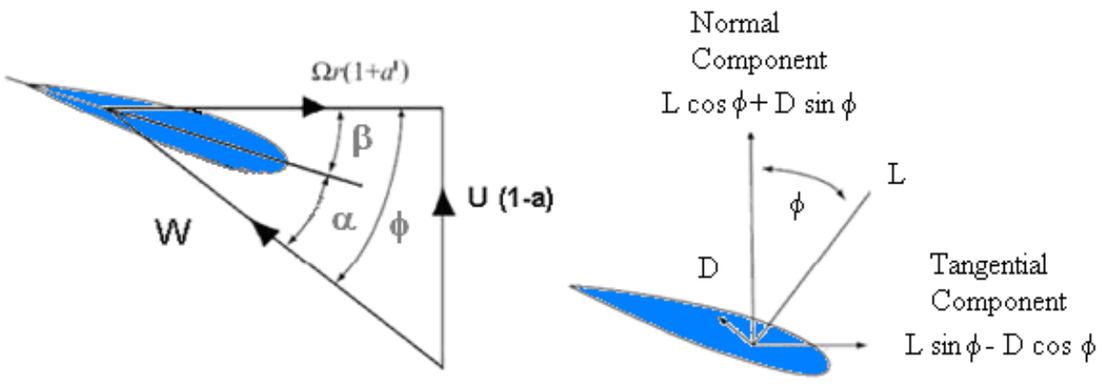

Fig. 7. Velocities and forces acting upon a blade-element

The differential torque will be:

$$\delta Q = r(\delta L \cdot \sin\phi - \delta D \cdot \cos\phi) \tag{17}$$

Such expressions will be employed to calculate the axial and tangential induction factors in the combined theory Blade-Element – Momentum in section 2.4.

2.3 Tip losses account

Due pressure on the blade´s upper surface (or suction side) is, in general, less than on the lower surface (high pressure side), air tends to move from the high pressure side to the lower pressure one (similar to a wing), producing a vortex system at the trailing edge called "trailing edge vortex system" which, combined with the pressure distribution on both sides, generate a lift distribution that tends to zero at the tips. All of that is responsible of the so called "tip losses", in a similar way than the airplane wing. Precisely, such 3D flow pattern is characteristic of a blade rotor or a wing, being the fluid dynamic difference between a wing and an airfoil in which the flow is 2D.

Stall is proper of 3D flow and can´t be determined by the blade-element theory. Nevertheless there are some physical models designed to include the tip losses. The most used of such models was developed by Prandtl (see also Glauert, 1935).

According such model a factor F is introduced in the equations to calculate net force and torque.

Such factor is a function of the number of blades B, effective pitch angle ϕ, blade element coordinate r and blade length, R.

Their mathematical empirical equation is:

$$F = \frac{2}{\pi}\cos^{-1}\left[\exp(-\frac{BR-r}{2r\sin\phi})\right] \tag{18}$$

2.4 Combined theory of momentum with blade element (BEM theory)

The purpose of this theory is to achieve a usable model to evaluate axial (a) and tangential induction factors (a´), from the equations for thrust and torque previously deduced by blade element theory. Now, the actuator disk will be an annulus of width δr and the differential lift and drag forces acting on it will be:

$$\delta L = \frac{1}{2}\rho \cdot W^2 \cdot c_L \cdot b \cdot \delta r \tag{19}$$

$$\delta D = \frac{1}{2}\rho \cdot W^2 \cdot c_D \cdot b \cdot \delta r \tag{20}$$

Replacing the previous equations in the [16] and [17] equations, results:

$$\delta Q = r \cdot \frac{1}{2} \cdot \rho \cdot W^2 \cdot b \cdot (c_L \cdot \sin\phi - c_D \cdot \cos\phi) \tag{21}$$

$$\delta F = \frac{1}{2} \cdot \rho \cdot W^2 \cdot b \cdot (c_L \cdot \cos\phi + c_D \cdot \sin\phi) \tag{22}$$

By other way we could express δF and δQ as:

$$\delta Q = r \cdot \frac{1}{2} \cdot \rho \cdot W^2 \cdot b \cdot c_Q \tag{23}$$

$$\delta F = \frac{1}{2} \cdot \rho \cdot W^2 \cdot b \cdot c_F \tag{24}$$

Equating the equations [8] and [16], for B blades, we obtain

$$2\rho A V_0^2 a(1-a) = B(l \cdot \cos\phi + d \cdot \sin\phi)R = BR\frac{1}{2}W^2 b \cdot C_F \tag{25}$$

Introducing solidity (σ) :

$$\sigma = \frac{B \cdot b \cdot R}{\pi \cdot R^2} = \frac{B \cdot b \cdot R}{A} = \frac{B \cdot b}{\pi \cdot R} \tag{26}$$

Being σ the relation between the area of B blades and the area described by the rotor; b is the blade chord.

So, with the help of the Prandtl correction factor, the induction factors will result:

$$a = \frac{1}{\frac{4 \cdot F \cdot \sin^2\phi}{\sigma \cdot c_F} + 1} \tag{27}$$

$$\acute{a} = \frac{1}{\frac{4 \cdot F \cdot \sin\phi \cdot \cos\phi}{\sigma \cdot c_Q} - 1} \tag{28}$$

2.5 Modifications to the above classical theory (BEM modifications)

Classic theory, developed in section 2.4, bring good results under operative conditions near specific velocity design, where specific velocity λ is the quotient between blade´s tangential tip velocity and free stream upwind velocity.

Nevertheless, for such specific velocity somewhat far from the design value, for example, for too high or too small λ values, classical theory didn´t give very good results. But, why is it so? Because the theory doesn´t take in account the 3D flow nature, turbulence, stall or losses.

In other words, classical theory work very good in situations where 3D flow is not too pronounced, but this isn´t always the situation and some modifications should be introduced to the theory.

Flow separation at the tip blade, promotes a downstream lowering of the static pressure Also, high static pressure appears on the stagnation zone of the blade. Such pressure

differences produce high thrust values on the blades that aren´t predicted by the classical BEM theory.

Glauert (1926, 1935) analyzed different induction factors (a) according flow pattern and propeller types. Spera (1994) proposed a rotor thrust taking in account the induction factor, a (see Figure 8).

According flow patterns, it´s possible to identify two different turbine states: one, called windmill or slightly charged state, is when turbulence doesn´t dominate flow field; the other, with high turbulence or high charged state, and classical BEM theory fails.

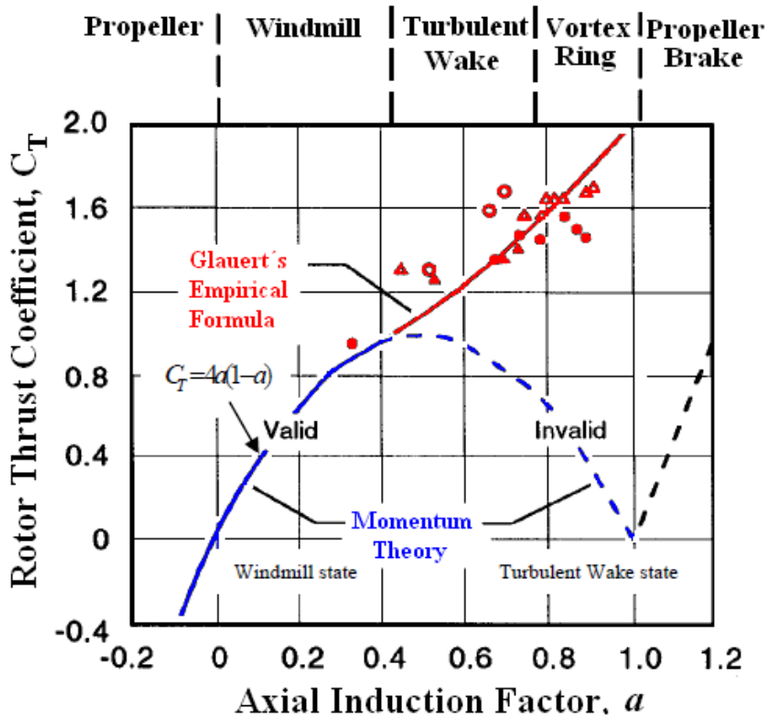

Fig. 8. Experimental and predicted C_T values

Phenomena described above could be included to the BEM theory, by different models: C_T and/or "a" predictions.

Glauert, in 1926, developed a correction for such phenomena employing experimental data from helicopters rotor blades. Such model was thought to correct overall thrust coefficient. Nevertheless, could be used to correct local thrust coefficient by means of the BEM theory.

Basically, Glauert corrections are related with tip losses model. When they grow up, also induced velocities so, hence the turbulence at the wake will increase. According that, the induced velocity calculus must take in account a combination of tip losses and Glauert correction.

Moriarty and Hansen (2005) in their book, explain the empirical Glauert relation modified with the tip losses factor.

The model is

$$C_T = \frac{8}{9} + (4F - \frac{40}{9})a + (\frac{50}{9} - 4F)a^2 \tag{29}$$

$$a = \frac{18F - 20 - 3\sqrt{C_T(50 - 36F) + 12F(3F - 4)}}{30F - 50} \tag{30}$$

2.6 Rotational effects upon aerodynamic coefficients

Himmelskamp (1947) investigated the increments of the maximum lift coefficients for rotating airplane propellers, assuming a radial flow downstream them. He found that such increment in the maximum lift is more pronounced for small radial sections, than the found values in the non rotation state at high angles of attack.

Other researchers have investigated the rotation effects for helicopters. Such investigations assume a local oblique flow at the rotor plane, during forward fly. In the work performed by Harris (1966), rotation effect is assumed by a yaw flow on the rotor plane. He reported that on calculating aerodynamic coefficients by conventional procedures, with a flow component normal to the blade axis, maximum lift also is enhanced with the oblique flow.

Fundamental aspects of the flow configuration in the model, is that the vorticity axis isn´t normal to the local flow direction and the separated flow is transported in the wingspan direction.

For forward flying helicopters, Dwyer & McCroskey (1970) offered a good description of the cross flow effects in the rotor blades plane.

At begin of the power control due aerodynamic stall in wind turbines, were observed that when such control actuated during stall, power tends to exceed the design value.

To describe rotational effects or delayed stall, various models were formulated, consisting the majority of them on add or extend lift coefficient without rotation. There are also few models which introduce corrections to the drag coefficient.

Some rotation effects correction models, are based upon pump air by centrifugal methods, over the separation bubble near trailing edge.

One of the first of such models was described by Sørensen (1986). In his work he showed flow patterns with radial configuration in the separation area around trailing edge.

His experimental results were reproduced, by himself and collaborators, by computational methods on S809 airfoil (Sørensen et all, 2002), which showed clearly centrifugal pumping at the trailing edge.

2.7 Centrifugal pumping mechanism

Centrifugal pumping on the separated air near trailing edge, originate radial flow. The result is that separation bubble size is diminished respect the situation of no-centrifugal loads. Due centrifugal load gradient, along wingspan, air pressure in the bubble is lower and, hence, normal force on the airfoil is enhanced.

At high angles of attack, pressure distribution on the upper surface of the airfoil, produce a suction peak just behind leading edge (leading edge suction force), which diminishes through the trailing edge. The magnitude of such force is proportional to dynamic pressure and, hence, it grows with the square of radial position.

Dynamic pressure gradient along wingspan and negative gradient along chord, conforms a mechanism responsible of the air, at the stall zone, flows to important radial coordinates and could overcome Coriolis forces.

Klimas (1986) describes radial flux by means of Euler equations, including centrifugal effects and Coriolis over separation bubble near the trailing edge.

After that, Eggers y Digumarthi (1992), and other authors, called such mechanism "centrifugal pumping".

Also was reported as "radial pumping" (Sørensen E.A., 2002) or "pumping along wingspan" (Harris, 1966).

Due centrifugal pumping on the separated mass flow around trailing edge, produce additional negative values to the pressure coefficient on the airfoil´s surface.

This extra "negative pressure" gives a negative gradient along chord which is favorable for the boundary layer stability and, in consequence, could shift separation point toward trailing edge. This change in the separation point is hard to model.

Nevertheless, we could assume that separation occurs at a higher angle of attack, being the pressure gradient along chord (included the increment due rotation effects) the same as the state without rotation.

Based upon that relation, it´s possible to elaborate correction models to take in account the increment of the angle of attack (delay).

In relation with such angle of attack change, lift coefficient should be extended in order to have the same slope between curves for totally attached flow (potential one) and totally separated.

Himmelskamp (1947) reported that if the lift stall coefficient, at high angles of attack, is delayed (or shifted), there aren´t observed drag coefficient increment.

Some physical models, which take in account rotation effects, are formulated upon hypothesis of "stall delay", like the ones of Corrigan and Schillings (1994).

2.8 Stall delay model by Corrigan and Schillings

Corrigan and Schillings (1994) developed a model to take in account correction effects upon rotation, expressed in terms of lift coefficients delay for high angles of attack.

The development of this method, begin with boundary layer equations following Banks & Gadd (1963).

Together with the expression for the boundary layer velocity gradient $\partial u / \partial z$, the delay amount was related with angular position of detachment point (θ_S). Precisely, problem formulation in terms of angular detachment point implies dependence between chord/radius relationships similar to other models.

One of the characteristic assumptions of the above cited model is that airfoil without rotation with maximum lift, could have a pressure suction peak at the leading edge, originating an important radial pressure gradient and, so, an important radial flux.

Due simplicity reasons, finally Corrigan and Schillings formulated their model in terms of the trailing edge angle θ_{TE}. For chord values not too big, that could be expressed in terms of the relation chord/radius (c/r).

Stall delay is expressed in terms of a change of the angle of attack, for lift coefficients without rotation:

$$\Delta\alpha = /\alpha_{CL\max} - \alpha_{CL=0}) \cdot ((\frac{K \cdot \theta_{TE}}{0.136})^n - 1) \tag{31}$$

Factor K describes the velocity gradient according the universal relation:

$$c/r = 0.1517 \ / \ K^{1.084} \tag{32}$$

For n = 0 (see equation [31]), the above formulas give aerodynamic coefficients without rotation. Corrigan established that for values of n between 0.8 and 1.6, there are a good correlation with the existing experimental data and, a value of 1 match with very good results in many situations. Authors like Tangler & Selig (1997) and Xu & Sankar (2002) used n=1.

The increment of lift coefficient (without rotation) is expressed in terms of the angle of attack increment, as:

$$C_{L.rot} = C_{L.non-rot(\alpha+\Delta\beta)} + (\partial C_L \ / \ \partial\alpha)_{pot} \Delta\alpha \tag{33}$$

Here, $(\partial C_L / \partial \alpha)_{pot}$ is the slope in the linear part of the polar lift coefficient vs. angle of attack. For such, Xu & Shankar used n=0.1.

2.9 Computational solvers

There were developed many CFD solvers for wind turbine blades design and, just for information only, we´ll mention 4 of them developed in USA, in a period of 15 years, presenting the evolution in the solvers content.

3. Aerodynamic airfoils

Airfoil to be selected on the rotor blade design, according our comments at Section 1, should satisfy requirements which are different than those used in the wing design for standard airplanes.

3.1 Reynolds number

Reynolds numbers upon blades are low and vary from the root to the tip. Table 2 shows typical Reynolds numbers corresponding to three turbine power levels, from root and tip. We could observe just only for wind turbines of big power (megawatt type), Reynolds number exceeds 10^6.

CODES Features	NUPROP AeroVironment	PROP93 AEI	PROPID Univ. of Illinois	AeroDyn NREL
Development Date	1986	1993	1997	2002
Airfoil Data Interpolation	no	no	yes	yes
3-D Stall Delay	no	no	yes	yes
Glauert Approximation	yes	yes		yes
Tip Losses	yes	yes	yes	yes
Windspeed Sweep	yes	yes	yes	yes
Pitch Sweep	yes	yes	yes	yes
Shaft Tilt	yes	yes	yes	yes
Yaw Angle	yes	yes	yes	yes
Tower Shadow	yes	no	yes	yes
Dynamic Stall	yes	no	no	yes
Graphics	no	yes	no	yes
Program Language	Fortran	C	Fortran	Fortran
Other	turbulence	hub ext.	Inverse design	The generalized dynamic wake theory

Table 1. Blade turbines CFD solvers time evolution in USA

Power	Re root	Re tip
50 kW	0.2 M	1.3 M
600 kW	0.7 M	1.3 M
2 MW	1.5 M	2.2 M

Table 2. Reynolds numbers for root and tip of wind turbines blades, for different power.

3.2 Low Reynolds number airfoils

First wind turbine developments used NACA airfoils like 4415, 4418, 23012, 23024, etc, which have good aerodynamic characteristics for higher Reynolds.

Boundary layer over a common airfoil, like NACA 4-digits series, under low angles of attack, have usually a favorable pressure gradient from the front stagnation point to approximately the maximum airfoil´s width, being the flow in most cases, laminar over such part. After the zone of minimum pressure, the pressure gradient changes its sign becoming unfavorable. Such sign change take place, in general, in a short distance.

Because that, for Reynolds number – based upon airfoil chord and mean free upstream velocity – below 5 x 10^5, boundary layer separate and again attach conforming a recirculation bubble on the upper surface of the airfoil. Such bubble could be short or long, depending on the perturbations present at the separation point and the local Reynolds number based upon boundary layer momentum thickness and local velocity, exactly before such point. See, for example, Chandrsuda & Bradshaw (1981) and Gad-el-Hak (2000).

Such changes in the flow on the upper surface affects negatively the lift generation. In fact, lift is especially sensible to any perturbation of the flow on the upper surface in higher

degree than on the lower surface. When boundary layer begins its detachment, conforming after that the mentioned recirculation bubble, the flow over detachment area becomes a shear layer which, downstream, evolution as a mix layer. Shear layer stability is particular sensible to velocity profile. The whole picture is a recirculation bubble with a shear layer on it, which could or not reattach (Ho & Huerre, 1984).

The main cause of bubble formation is the almost abrupt change in the pressure gradient on the upper surface, from favorable to unfavorable in a small extension. To minimize those adverse effects, appeared the low Reynolds number airfoils (Zaman y Hussain, 1981), (Eppler y Somers, 1980), (McGhee y Beasley, 1973), (Eppler, 1990), (Carroll, Broeren, Giguere, Gopalarathnam, Lyon and Selig, 1990-2000), being their main characteristic the gradual change of pressure gradient sign from negative to positive in a larger extension than the standard airfoils, for a $5x10^4 \leq Re \leq 5x10^5$ range. So, a better lift distribution was achieved.

Nevertheless, all mentioned airfoils designs were tested in laminar flow wind tunnels, but the real condition of the flow where are wind turbines operate is in general turbulent, that´s, the flow corresponding to the low atmospheric turbulent boundary layer. Some researchers, like Delnero et al (2007), have performed experiments in boundary layer wind tunnels, with low Reynolds airfoils. They studied the flow field at the neighbor of the airfoil and, in particular, how is the bubble formation and evolution, under turbulent free upstream.

Some wind turbine builders, apart from low Reynolds airfoils, tested laminar airfoils like NASA LS(1)_0413 MOD but, due their high sensibility to roughness their required repeatedly clean due insects upon blade surface.

For such reason, researchers realized that one of the most important characteristic of the airfoils to be used on rotor blade design, should be those with less sensibility to roughness changes during their operation, by dust and/or insects on the leading edge area.

Research performed in USA and Europe leave to design of new airfoils families which are less sensible to roughness changes.

For example, the National Renewable Energy Laboratory (NREL, USA) designed the airfoils S8xx for different blade sizes.

Other Universities like Illinois (USA) and Delft (Netherlands) was also contributed to such type of airfoils design.

Du structural reasons, blade root should be of great width in order to increment inertia moment and resist better the moments. By other side, tip blade must have small width because it moves to high velocity. For that, a typical blade airfoil family goes from great width at the root to small width at the tip. Table 3 is indicative about that.

Airfoil	r/R	t/c (%)
tip region	0.95	16
primary outboard	0.75	21
roof region	0.4	24

Table 3. Airfoils with different width along blade wingspan

3.3 Selection criteria of airfoils and rotor blade design

To airfoil election to be used on a rotor blade, we should take in account:

1. From moderate to high relative width (t/c), for a rigid rotor, such relation could be between 16% and 26%. If the rotor were flexible, the relative width should lie between 11% and 16%.
2. 2D Reynolds number of the airfoils should be the appropriate to the design considerations.

Fig. 9. Wind turbines (WT) of different powers, exhibiting aerodynamic different solutions; (top at the left side) WT of 600kW in the wind farm Bajo Hondo in Punta Alta, Argentina, with brake in tip of blade; (top at the right) small WT of 1kW for autonomous supply of relay station of micro waves in surroundings of Puerto Madryn, Argentina; (below) blade of WT of 2 MW in Magdalena's wind farm (Uruguay).

3. Less roughness sensibility is of primary importance due wind turbine stall regulation.
4. Lift budget for minimum drag and C_{lmax}: should be designed for a determinate lift range for minimum drag, despite that for small wind turbines drag acts as passive flow control and have a relative influence upon their function.
5. High lift root airfoils, in order to reduce as much as possible solidity and to increment the starting torque.

For example, Figure 9 show us three wind turbines under operation in different places, for small, medium and high power and, consequently, with different aerodynamic solutions. The first two are located in Argentina and the last one in Uruguay.

Also should be taken in account:

1. Low lift values implies greater solidity and aerodynamic loads.
2. Extreme aerodynamic loads are particularly important for great wind turbines.
3. Low lift airfoils have a smooth stall, which is dynamically positive and the power peaks are reduced.
4. High lift implies small chord values and low operational Reynolds numbers, with subsequent building difficulties.
5. Reynolds number effects are particularly important for small wind turbines.
6. Rotor solidity should be optimal, remembering that´s defined by the relation between blade area and area covered in one complete rotation:

$$\sigma = \frac{Blade\ Area}{\pi \cdot R^2} \tag{34}$$

Low solidity values are related, commonly, with low weight blades and low overall cost

For a given maximum power, optimal solidity depends upon: rotor diameter (big diameter imply low solidity); aerodynamic airfoil (for example, high C_{lmax} imply low solidity); rpm of the rotor (for example, high rpm imply low solidity); blade material (for example, carbon fiber imply low solidity).

4. References

Banks,W.H.H. and Gadd, G.E.; "Delaying effects of rotation on laminar separation". AIAA Journal Vol.1, No.4, Technical note, pp.941-942, 1963.

Carroll C.A., Broeren, A.P., Giguere,P , Gopalarathnam,A , Lyon C.A, and. Selig; M.S; "Low Reynolds Number Airfoil Design and Wind Tunnel Testing"; UIUC, 1990 - 2000

Chandrsuda C. and Bradshaw P.; "Turbulence structure of a reattaching mixing layer". Journal of Fluid Mechanics Vol. 110, pp. 171-194; 1981.

Corrigan, J.J. and Schillings, J.J.; "Empirical Model for Stall Delay due to Rotation". American Helicopter Society Aeromechanics Specialists conf, San Francisco CA, Jan. 1994.

Delnero, Sebastián; "Comportamiento Aerodinámico de Perfiles de Bajo Reynolds, Inmersos en Flujo Turbulento"; Tesis Doctoral, Universidad Nacional La plata; 2007.

Dwyer, H.A. (univ of Calif., Davis) and Mc Crosky,W.J.; "Crossflow and Unsteady Boundary-layer Effects on Rotating Blades". AIAA paper no.70-50, pp.1-15, January 1970.

Eggers, A.J. and Digumarthi, R.; "Approximate Scaling of Rotational Effects of Mean Aerodynamic Moments and Power Generated by the Combined Experiment Rotor Blades Operating in Deep-Stalled Flow". 11-th ASME Wind Energy Symposium, Jan. 1992, pp.33-43.

Eppler, R., and D.M. Somers; "A Computer Program for the Design and Analysis of Low Speed Airfoils"; Technical Memorandum 80210, NASA, Aug. 1980.

Eppler, Richard; "Airfoil Design and Data" . Springer - Verlag , Berlin, 1990.

Gad-el-Hak, M. (2000). "Flow control: Passive, Active and Reactive Flow Management". Cambridge Univ. Press. ISBN 0 521 77006 8.

Glauert, H. (1926). "The Analysis of Experimental Results in the Windmill Brake and Vortex Ring States of an Airscrew", Rept. 1026. Aeronautical Research Committee Reports and Memoranda, London: Her Majesty's Stationery Office.

Glauert, H. 1926. "A General Theory of the Autogyro." *ARCR R&M No. 1111.*

Glauert, H. 1935. "Airplane Propellers." Aerodynamic Theory (W. F. Durand, ed.), Div. L, Chapter XI. Berlin:Springer Verlag.

Harris, F.D. (Vertol Division, The Boeing Company, Morton, Pennsylvania); "Preliminary study of radial flow effects on rotor blades". Journal of the American Helicopter Society, Vol.11, No.3, pp.1-21, 1966.

Himmelskamp, H. (PhD dissertation, G¨ottingen, 1945); "Profile investigations on a rotating airscrew". MAP Volkenrode, Reports and Translation No.832, Sept. 1947.

Ho C.M. & Huerre P.; "Perturbed free shear layers". Annual Review of Fluid Mechanics 16, pp. 365-424; 1984.

Klimas, Paul C.; "Three-dimensional stall effects". 1-st IEA Symposium on the Aerodynamics of Wind Turbines, London, 1986, pp.80-101.

McGhee, R. J., and W. D. Beasley; "Low - Speed Aerodynamics Characteristics of a 17 - Percent - Thick Section Designed for General Aviation Applications", TN D-7428 NASA, Dec. 1973.

Moriarty P. J., Hansen C. A.,"AeroDyn Theory Manual", NREL EL/-500-36881, December 2005.

Spera, D.A. (Ed.): "Wind Turbine Technology",ASME Press, New York, 1994.

Sørensen, Jens Nørkaer; "A new computational model for predicting 3-D stall on a HAT". 1-st IEA Symposium on the Aerodynamics of Wind Turbines, London 1986.

Sørensen, J.N., Michelsen, J.A., and Schreck, S.; "Navier-Stokes predictions of the NREL Phase-IV rotor in the NASA Ames 80-by-120 wind tunnel". AIAA-2002-0031, ASME Wind Energy Symposium, 2002, pp.94-105.

Tangler, J.L. and Selig, Michael S.; "An evaluation of an empirical model for stall delay due to rotation for HAWTs". In ProceedingsWindpower '97, Austin TX, pp.87-96.

Xu, Guanpeng and Sankar, Lakshmi N.; "Application of a viscous flow methodology to the NREL phase-IV rotor". ASME Wind Energy Symposium, Reno 2002, AIAA-2002-0030, pp.83-93.

Zaman K.B. & Hussain A.K.; "Turbulence suppression in free shear flows by controlled excitation". Journal of Fluid Mechanics 103, pp. 133-159; 1981.

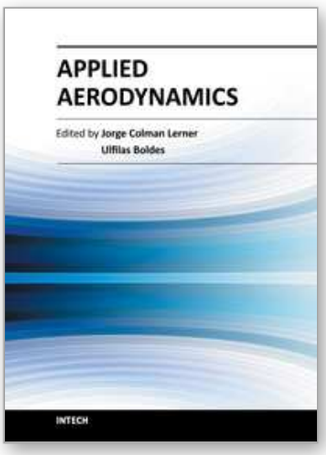

Applied Aerodynamics

Edited by Dr. Jorge Colman Lerner

ISBN 978-953-51-0611-1

Hard cover, 192 pages

Publisher InTech

Published online 11, May, 2012

Published in print edition May, 2012

Aerodynamics, from a modern point of view, is a branch of physics that study physical laws and their applications, regarding the displacement of a body into a fluid, such concept could be applied to any body moving in a fluid at rest or any fluid moving around a body at rest. This Book covers a small part of the numerous cases of stationary and non stationary aerodynamics; wave generation and propagation; wind energy; flow control techniques and, also, sports aerodynamics. It's not an undergraduate text but is thought to be useful for those teachers and/or researchers which work in the several branches of applied aerodynamics and/or applied fluid dynamics, from experiments procedures to computational methods.

How to reference

In order to correctly reference this scholarly work, feel free to copy and paste the following:

J. Lassig and J. Colman (2012). Wind Turbines Aerodynamics, Applied Aerodynamics, Dr. Jorge Colman Lerner (Ed.), ISBN: 978-953-51-0611-1, InTech, Available from: http://www.intechopen.com/books/applied-aerodynamics/wind-turbines-aerodynamics

INTECH
open science | open minds

InTech Europe
University Campus STeP Ri
Slavka Krautzeka 83/A
51000 Rijeka, Croatia
Phone: +385 (51) 770 447
Fax: +385 (51) 686 166
www.intechopen.com

InTech China
Unit 405, Office Block, Hotel Equatorial Shanghai
No.65, Yan An Road (West), Shanghai, 200040, China
中国上海市延安西路65号上海国际贵都大饭店办公楼405单元
Phone: +86-21-62489820
Fax: +86-21-62489821

IntechOpen